Operationalize The Meridian Imaging Svalbard Spectrograph (MISS) II

Author: Jesse Delbressine 1598015

Supervisor UNIS: Fred Sigernes
Supervisor TU/e: Hjalmar Mulders

Abstract

In winter 2018 the Meridian Imaging Svalbard Spectrograph 1 (MISS 1) went into operation at the Kjell Henriksen Observatory(KHO) in Longyearbyen, Svalbard. This hyperspectral imager is capable of tracking auroral emissions along the geomagnetic meridian. It is able to capture wavelengths in the visible spectrum with high spectral resolution. Wanting to perform comparisons between multiple hyperspectral imagers located approximately 100 kilometres apart led to development of MISS 2. It is roughly the same as MISS 1 but the design is a bit sturdier. The design of MISS 1 and 2 is straightforward, using a tunable grating in combination with a prism (tGRISM) as a dispersive element, some basic optical elements and no moving parts making them low maintenance devices which makes them perfect for operating at an unmanned observatory such as KHO (and eventually at Ny-Ålesund).

This project focuses on operationalizing MISS 2 by enhancing the software such that it is able to captures spectrograms continuously, process them immediately and publish the relevant data and graphs on the KHO website without human interference. These improvements allow MISS 2 to operate autonomously throughout the auroral season. The upcoming season will serve as a test phase to fine-tune the parameters and settings for optimal aurora tracking performance.

Contents

1 Introduction

Aurora borealis was one of the large mysteries in the history of science. The name aurora borealis was coined by Galileo Galilei, meaning "dawn of the north" [1]. In the early 1700s some exceptional views of aurora were visible over almost the whole of Europe, even in Spain it could be seen. For many people this phenomenon was a natural wonder which was often linked to superstition. Several natural philosophers tried to make sense of this weird phenomenon through performing research and integrating it into the framework of mechanistic natural philosophy. Many questions remained: was it the result of sun-or moonlight reflection, was it an electrical or chemical effect, occurred it due to volcanic activity in the vicinity and why did it happen at certain locations [2]?

Around the 1850s a lot of the fancy and wild theories about the aurora had been proved wrong by performing experiments and rational thinking. However, there still hadn't been consensus by the researchers on the cause of the auroras. Some argued that it was due to friction between ice crystals that would form local electrical discharges and others were convinced that it was the caused by space dust. In the early 1900s Kristian Birkeland proposed a theory in which he linked auroras to solar wind, which are charged particles emitted by the sun. These charged particles would then interact with the Earth's magnetic field. The particles would then be directed towards the polar regions and form auroras. His theory was made fun of in his time but is nowadays widely accepted [3] [4].

In more detail, the sun continuously releases a stream of charged particles (the solar wind), i.e. protons and electrons. This flow is constant and can vary in intensity. When the protons and electrons reach the earth most of them are deflected by the earth's magnetic field but some can enter. The ones that enter will flow to the atmosphere near the magnetic poles since the magnetic field lines converge at the poles. The particles will interact/collide with the gases present in the atmosphere, nitrogen and oxygen. Due to these collisions the protons and electrons will transfer energy to the nitrogen and oxygen which will excite them and when they return to their normal state they will emit light which can be observed and as the phenomena known to most of the population, Aurora Borealis or more commonly Northern (or Southern) lights [1] [5] [6]. Most of the Aurora seen by humans have a green colour. This is due to the oxygen at lower altitude (around 100km). However, at higher altitude the oxygen can produce a red colour and at really low altitude the nitrogen can create a blue colour [1].

Figure 1.1: Aurora Borealis above Sukkertoppen Longyearbyen, Svalbard.

Auroras can be investigated using several methods such as ground-based observations i.e. optical zoom camera and spectrometers, space-based observations i.e. satellites and theoretical and computational models [7] [8]. In this report a spectrograph is operationalized in order to investigate auroras, in particular hyperspectral imagers (HSI). A HSI will combine the fields of spectroscopy and imaging by capturing spatial and spectral information simultaneously. A normal spectral imager or a multispectral imager also captures spatial information and spectral information, but the pixels in such a multispectral imager can often only register a RGB (Red Green Blue) coordinate. A HSI can register the spectral information with much higher resolution by capturing the light in many narrow bands, in stead of only three, across a broad range of wavelengths [9]. So, it can detect minor differences in the wavelengths of light. The HSI will capture 2 dimensions of spatial information (x, y) and one dimensions of spectral information (λ) which it will store in a three dimensional cube (x, y, λ) [10]. See figure 2.7 for such a datacube.

In the early 70s the first field spectral measurements were performed and the scientific world started to see the promise of spectrometry. These experiments gathered a lot of data which could not or barely be handled by the computers and data centres back then. And this was when they used only three spectral bands. Furthermore, using more bands than these three seemed a bit redundant since no material required several hundred of spectral bands to be identified. However, once the data storage capacity and computing power were good enough researchers started to see the benefits of having several hundreds of spectral bands since they could then identify almost every material with great precision. It can be said that the development of hyperspectral imagers is closely related to the advancements in microelectronics [11].

The hyperspectral imager used in this report is the so called Meridian Imaging Spectrograph 2 (MISS 2). It is used since the goal is to track aurora and the best way to do that is to look along the magnetic field lines which are converging towards the magnetic poles, since it is expected that the chance of observing aurora is highest around the magnetic poles. In order to track them a wide field of view is needed and it is best to observe along the geomagnetic meridian plane from North to South. Note: a meridian is a line running from the geographic North to South Pole and the magnetic poles are different from the geographic poles. Therefore, the earth's magnetic field lines will converge towards the magnetic poles and not the geographic poles. Thus, the geomagnetic meridian plane is an imaginary plane going through the earth parallel with the earth's magnetic field.

The MISS used in this report has been installed and operated at the Kjell Henriksen Observatory (KHO), see figure 1.2. KHO is an optical observatory located in Svalbard, which is around 1000km North of Tromsø. There are roughly 30 optical instruments used for research into middle- and upper atmosphere. The instruments are placed in the instrument rooms consisting out of a instrument/dome room and a control room.

Figure 1.2: Picture of the KHO, taken after installing MISS 2. On top of the building the domes where the instruments are placed in can be seen.

The main focus of this study is to operationalize the MISS 2 at the KHO such that it can be used independently and run continuously for the coming auroral season. The ultimate goal is to let MISS 1 (similar to MISS 2 but a bit less sturdier design) and MISS 2 run both on the software developed by Nicolas Martinez and the author and place MISS 1 at Ny-Ålesund (approximately 100 kilometres away from KHO) such that a triangle is made and also height measurements and comparisons can be done. In chapter two some basic theory about imaging optics and spectral imaging is given, in chapter 3 the hardware and software of MISS 2 is discussed, in chapter 4 some obtained results are given and lastly the conclusions are drawn and a small discussion is held.

2 Theory

In order to explain how MISS 2 works first some basic knowledge of imaging optics and hyperspectral imaging is needed. Therefore, this section provides a basic description of these concepts. In the first part a basic introduction to spectroscopy is given, then the characteristics and properties of light are discussed, some relevant terminology is given and the imaging system is discussed. Then a short description of hyperspectral imaging is given after which some information about the calibration sequence is given and lastly the characterization of the system is discussed. In the theory presented the following sources have been used; [12], [13]

2.1 Basic Spectroscopy

In simple terms, a spectrograph will take up light, split it up by wavelength and create a spectrum displaying the intensity of light as a function of wavelength. In order to know exactly how it works first some basic properties of light are explained.

2.1.1 Properties of light

Light can be described as both a particle and a wave which led to the wave-particle duality. This means that light can be viewed as packets of photons exhibiting electromagnetic wave-like properties. This wave can be defined as

$$E(\mathbf{r}, t) = E_0 \sin(\mathbf{k} \cdot \mathbf{r} \pm \omega t) \tag{1}$$

where $E(\mathbf{r}, t)$ is the amplitude of the wave, E_0 the maximum amplitude of the wave, $\mathbf{k} = \frac{2\pi}{\lambda}$ is the propagation number with λ the wavelength, $\mathbf{r}$ is the position of the wave, $\omega = 2\pi f$ the angular frequency and the wave is periodical in time t with period $T = \frac{\lambda}{c}$ where c is the speed of light.

To trace and understand the behaviour of light travelling through an imaging system geometric optics is used. And to simplify it even more the paraxial approximation has been used. A paraxial ray makes only a small angle with the optical axis ($\theta < 5$ degrees) which means that the direction of the rays will only be changed by reflection and refraction. So, when using a Taylor expansion for $\sin(\theta)$ the following is found:

$$\sin\theta \approx \theta - \frac{\theta^3}{3!} + \frac{\theta^5}{5!} - ..., \tag{2}$$

and thus for small angles the following relations will hold:

$$\sin\theta \approx \theta, \ \cos\theta \approx 1 \ \text{and} \ \tan\theta \approx \theta. \tag{3}$$

Interference and Diffraction

Interference is a phenomena which happens when two waves superimpose to form one resulting wave which has higher, lower or the same amplitude as the originals waves (when the phases of the original waves differ with 90 degrees). Diffraction occurs when a wave is distorted by an obstacle. Note: the object has to be of comparable dimensions as the wavelength of the wave. See figure 2.1. More on the diffraction grating used can be found in section 2.1.3
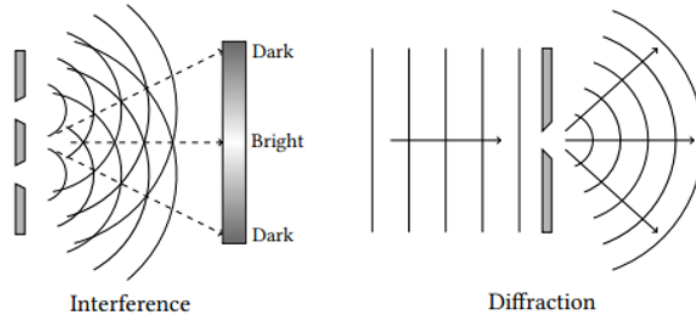
Figure 2.1: On the left hand side two waves interacting resulting in an interference pattern and on the right hand side diffraction due to a wave hitting an obstacle. Illustration is adapted from [14].

2.1.2 Definitions

In the optics field a lot of terminology is used with slightly different meaning and units. In order to distinguish them all they are introduced below.

Solid Angle

The solid angle can be defined as

$$\Omega = \frac{A}{r^2} \tag{4}$$

where r is the radius of the sphere, A is the spherical surface area and the solid angle Ω has units steradians (or square radians) [sr]. An illustration of solid angle can be seen below.
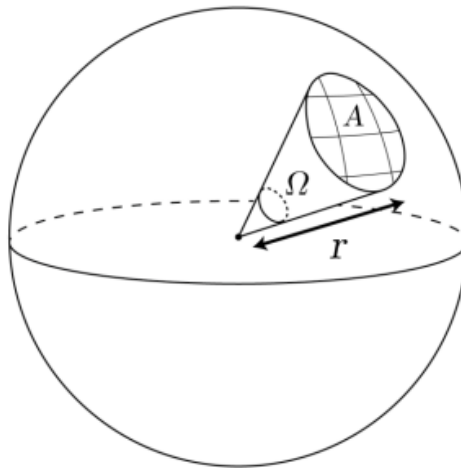
Figure 2.2: Definition of Solid angle, illustration from [15].

Radiant flux

The radiant flux, Φ_r is defined as the number of radiant energy emitted from a source into a solid angle per unit time. It can also be defined as the number of photons emitted per unit of time into a solid angle.

$$[\Phi_r] = \frac{J}{s} = W. \tag{5}$$

Intensity

The intensity, I, is linked to the radiant flux since intensity is radiant flux per unit solid angle or radiant energy emitted per unit time squared and solid angle.

$$[I] = \frac{J}{s\ sr} = \frac{W}{sr}. \tag{6}$$

Radiance

The radiance, B, is linked to the flux as well since radiance is radiant flux per unit solid angle and area or radiant energy emitted per unit time squared, solid angle and area. The spectral radiance, B_λ, is the radiance per wavelength.

$$[B] = \frac{J}{s\ sr\ m^2} = \frac{W}{sr\ m^2} \quad \text{and} \quad [B_\lambda] = \frac{W}{sr\ m^2\ nm}. \tag{7}$$

Irradiance

The irradiance, E, is the radiant flux hitting an surface area per unit area. The spectral irradiance, E_λ is the irradiance per wavelength.

$$[E] = \frac{W}{m^2} \quad \text{and} \quad [E_\lambda] = \frac{W}{m^2 nm}. \tag{8}$$

2.1.3 Imaging System

An example of an optical diagram can be seen in figure 2.3, in such a diagram the rays through a spectrograph can be traced. Light from the source S will reach the first lens L_1, also called front lens, which will focus the light onto the image source area S_1. Then the light which passes through the entrance slit area S_2 will be collimated by lens L_2 onto the dispersive element G which can be a grating, prism or a combination of both. This dispersive element will split the light depending on the wavelength in such a way that the centre wavelength will be in the middle and parallel to the optical axis. The last lens will then focus the light onto the sensor S_3 which will make a spectrogram out of the light. Which will have one axis the spectral information and on the other axis the spatial information.
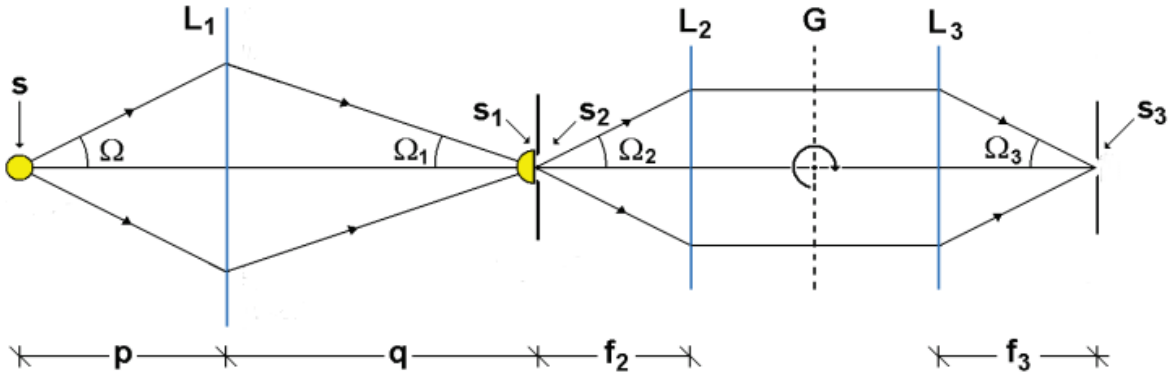
Figure 2.3: Optical diagram of a spectrograph consisting out of several components. S area of light source, $\Omega, \Omega_1, \Omega_2$ and Ω_3 are the half angles. L_1, L_2 and L_3 are the lenses. G is the dispersive element, S_1 is the imaged area, S_2 is the entrance slit area and S_3 is the sensor. p is the object distance, q is the image distance of lens L_1, f_2 is the focal length of lens L_2 and f_3 the focal length of lens L_3. Figure adapted from [13].

Focal length

Converging rays close to the optical axis will come together in one point on the optical axis, which is called the focal point. The distance from the centre of the lens to the focal point is the focal length f. Using the thin lens approximation makes ray tracing easier and optical effects due to thickness of lens are ignored. Note: for a lens to be called thin its thickness should be much smaller than the radii of the curvature of the lens.

$$\frac{1}{f} = \frac{1}{p} + \frac{1}{q} \tag{9}$$

Here f is the focal length, p is the object distance and q is the image distance. The ability of an imaging system to gather light is defined by the f/value or f/#. It can also be referred to as the speed of the lens.

$$f/\# = \frac{f}{D} \tag{10}$$

Where D is the effective aperture of the system. So, lower f/# values mean that the system's ability to gather light is better. The field of view (FOV) defines the observable area which an optical system (or a lens) can capture, which is often expressed in degrees. For example, if the FOV is 50 degrees then the optical system can capture everything within a 50 degree cone. Relating this to focal length; a long focal length means a smaller/narrower FOV and a short focal length means a larger/wider FOV.

Geometric Extent

Étendue or geometric extent describes the ability of a system, often optical systems, to accept light. It also describes the flux transfer ability of the system. Étendue G is the product of the area S of the emitting source and the solid angle C. Note: C is used here for the solid angle instead of Ω to prevent confusion and Ω is the half angle as seen in figure 2.3.

$$G = \iint dSdC. \tag{11}$$

Integrating this equation gives $G = S \cdot C$. Using equation 2.1.2 and figure 2.3 the solid angle becomes:

$$C = \frac{A}{r^2} = \frac{\pi r^2 \sin^2 \Omega}{r^2} = \pi \sin^2 \Omega. \tag{12}$$

The geometric extent becomes then:

$$G = S \cdot C = S\pi \sin^2 \Omega. \tag{13}$$

Geometric extent can never decrease in an optical system where conservation of optical power applies, however it can decrease when there is loss of light due to geometric blocking, scattering etc. So, an optimally constructed instrument is wanted such that:

$$G = S\pi \sin^2 \Omega = S_1\pi \sin^2 \Omega_1 = S_2\pi \sin^2 \Omega_2 \tag{14}$$

and thus the geometric extent is optimized.
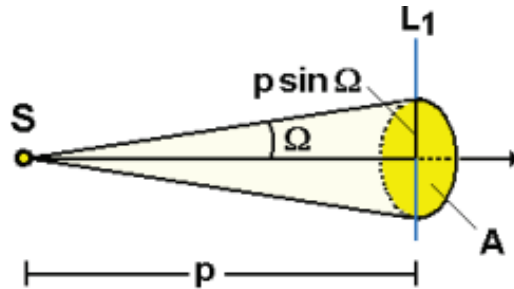
Figure 2.4: The geometric extent of the front lens in which S is the light source, L_1 the front lens, Ω the solid angle where the light is allowed to travel and p is the object distance. Figure from [13].

Grating

In this section the following book has been used [16].

The dispersive element is a key element in the spectrograph since it will split the light depending on the wavelength. The element can be a grating, prism or a grism (a combination of a grating and a prism). A diffraction grating is a N-slit aperture which will create a diffraction profile/interference pattern with principle maxima. The slits have a distance d between them and width b. The light falling on the grating will be diffracted according to the diffraction equation, see equation 2.1.3.

$$m\lambda = d(\sin\alpha + \sin\beta) \tag{15}$$

Here m is the diffraction order which must be an integer value, λ is the wavelength, α is the light's incident angle and β is the diffracted angle of the light. When $m = 0$ the light is not diffracted but directly reflected or transmitted by the grating. So, the maxima of all wavelengths are given at the same diffracted angle β. For $m = 1$ and higher orders β will vary with wavelength, so the maxima are not at the same location but varying with wavelength. When using a grating, light with smaller wavelength will have a smaller refracted angle β than light with longer wavelength, so blue light will have smaller refracted angle than red light. When using a prism this will be the other way round.
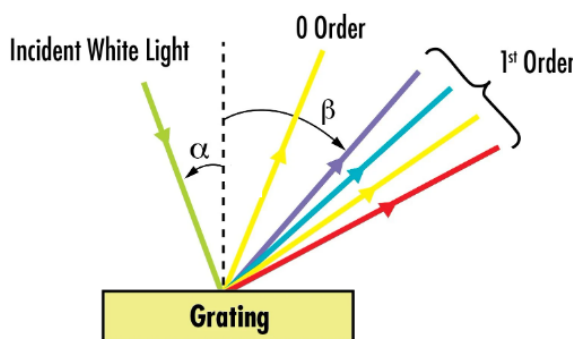
Figure 2.5: A diffraction grating with several orders of diffraction. Figure adapted from [17].

The zeroth order has the maximal intensity but as seen in figure 2.5 it only reflects/transmits the light. Since the separation of wavelengths is wanted the next best order is the first order, however here the intensity already goes down. In order to have the first order with maximal intensity a blazed diffraction grating can be used. This is a grating whereby the reflective surfaces are tilted a bit at an blaze angle ω_b, see figure 2.6. The shift of the maximum intensity from zeroth order to first order will be most effective when

$$\alpha - \omega_b = \omega_b + \beta. \tag{16}$$

Combining this with equation 2.1.3 the wavelength for which the grating has the highest efficiency, blazed wavelength, is found:

$$\lambda_b = \frac{2d}{m}\left(\sin(\alpha) + \sin(\alpha - 2\omega_b)\right). \tag{17}$$
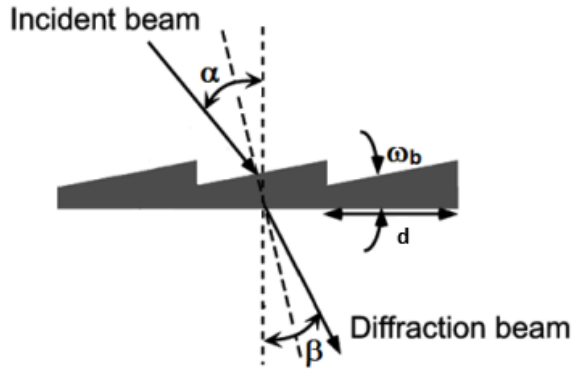
Figure 2.6: Blazed grating with blazed angle ω_b. Figure adapted from [18].

2.2 Hyperspectral Imaging

Hyperspectral imaging (HSI) is a imaging technique which combines the fields of imaging and spectroscopy. HSI provides precise information about the properties and composition of the material it is capturing. It does this by capturing light of a wide spectrum in many narrow bands across a broad range of wavelengths, mostly in the visible and near-infrared region. So a HSI does not capture a RGB (Red Green Blue) coordinate but a whole spectrum of wavelengths. Thus, instead of collecting three bands several hundreds of bands are collected such that every wavelength in the spectrum is covered and a continuous spectral band is obtained. The HSI captures spatial information in two dimensions, (x, y), and in one dimension spectral information (λ). This information/data will be stored in a so-called hyperspectral cube. Here the spatial data is stored in the first two dimensions and the spectral in the third dimension, so a three dimensional cube (x, y, λ) will be captured. See figure 2.7 for such a hyperspectral cube.
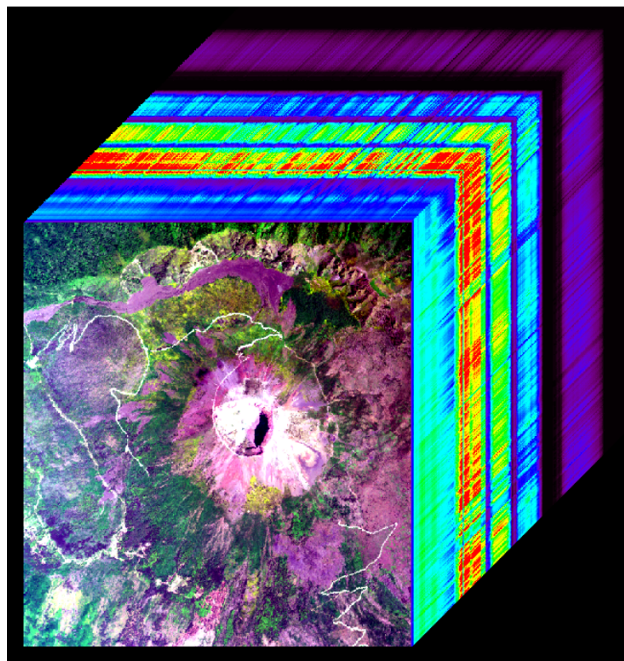
Figure 2.7: A hyperspectral cube from Mount Vesuvius in Italy, figure from [19].

2.2.1 Pushbroom Method

There are several methods to obtain such a hyperspectral cube, one of the most common one is pushbroom scanning techniques. For pushbroom the imager is designed is such a way that the optical slit is perpendicular to the scanning direction. For MISS2 pushbroom will be used. Here one line of spatial direction is captured together with the spectral information at a given moment in time. Then the imager is moved, for example by attaching the HSI to a moving table or flying plane, and a new line with spatial and spectral information is obtained. This process will continue for a certain amount of time and then all the obtained 2D images are then put together to form a 3D hyperspectral cube. See figure 2.8 for an illustration.

But, MISS2 will not be attached to a plane instead the image it captured is now moving, i.e. the sky is captured which is moving over time so to speak. So, then it will also capture three dimension over time forming a hyperspectral cube.
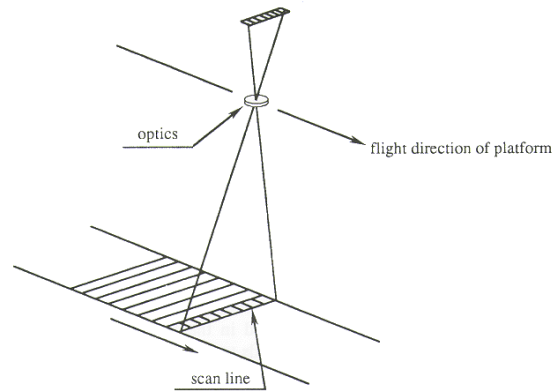
Figure 2.8: The pushbroom scanning technique. Figure from [20].

2.3 Calibration

Calibration is the act of setting parameters of an instrument by comparing the performance of the instrument with known standards. For a hyperspectral imaging device two calibrations need to be performed, first a wavelength or spectral calibration and then a radiometric calibration.

2.3.1 Wavelength Calibration

Wavelength calibration provides a relationship between the recorded spectral data by the pixel and the corresponding wavelength value. The basic method is to use several spectral lamps with peaks with known wavelengths (the peaks have to be in the range of the detector). The HSI will obtain images of the spectrum projected by the lamp. The known wavelengths of the lamp are then related to the measured peaks which will then give a relationship between the two. This relation is called the wavelength pixel relation. Here the pixel positions are linked to wavelengths, see equation below.

$$\lambda(x) = a_0 + a_1 \cdot x + a_2 \cdot x^2 + \cdots + a_n \cdot x^n \tag{18}$$

Here x is the pixel position, a_0, a_1 and a_2 are the calibration coefficients and $\lambda(x)$ is the wavelength depending on the pixel position. The goal of this calibration is to find coefficients such that the wavelength can be determined by only knowing the position of the pixel. The method for obtaining these coefficients is as follows; gather the data from the calibration lamps that emit light at specific known wavelengths. Then identify the pixel position for the known wavelengths. For example: it is known that one calibration lamp emits light at 550nm and the observed peak appears at pixel $x = 300$, thus pixel 300 corresponds to 550nm. Do this for multiple known wavelengths and a polynomial can be fit through the data. Lastly, validate the coefficients by comparing the determined wavelengths by the polynomial with the actual known wavelengths

of the calibration lamps.

2.3.2 Radiometric Calibration

Radiometric calibration or sensitivity calibration is the relation between the detected signal and actual radiance. So, find a relation between raw number of electronic/sensor count (detected signal) and the actual radiance. Thus converting raw data (electronic counts) into radiance since radiance has more physical meaning units. The goal is to find the calibration factor K_λ for the individual pixels and use the background corrected sensor counts to convert the digital counts to the correct radiance value at each pixel. The calibration factor is given below:

$$k_\lambda = \frac{M_\lambda}{C} \tag{19}$$

where M_λ is the radiant existence of the screen and C background corrected sensor count counts per second of the lamp. K_λ has units $\frac{\mathrm{mW}}{\mathrm{m^2\ sr\ nm\ counts}}$. M_λ of a diffuse screen represents its brightness as perceived by an instrument and can determined using the equation below:

$$M_\lambda = B_{0\lambda}\rho_\lambda \left(\frac{z_0}{z}\right)^2 \cos\alpha \tag{20}$$

where $B_{0\lambda}$ is the known radiance of the calibration lamp, ρ_λ is the reflectance factor of the screen, z_0 is the distance at which the known radiance $M_{0\lambda}$ is obtained, z is the distance at which M_λ is obtained (this is given by the supplier) and α is the angle between the lamp and the diffusive screen. In order to determine the background corrected sensor count of the lamp C, the dark current b_0 must be subtracted from the raw electronic counts. The dark current can be obtained when one measures the number of counts with no illumination. Note: these calibrations have been done by Nicolas Martinez, his thesis is not yet published.

2.4 Characterization

Characterization is the act of describing distinctive characteristics of the imager in order to understand the system more and assess its performance.

2.4.1 Spectral Bandpass

Spectral bandpass (BP) refers to ability of an optical instrument to distinguish between (closely) spaced spectral lines. Often it is determined as the Full Width at Half Maximum (FWHM) of a recorded monochromatic spectral line [13]. The spectral bandpass can be determined theoretically using the following equation:

$$BP = FWHM \approx \frac{d\lambda}{dx} \cdot w'. \tag{21}$$

Here $\frac{d\lambda}{dx}$ is the linear dispersion which describes how the wavelength changes with respect to distance along the sensor (changing of pixel). So, each unit of distance along the sensor (each pixel) corresponds to a constant change in wavelength. And w' is the width of the exit slit.

Angular dispersion refers to the rate of change in the diffracted angle of light with respect to the wavelength, so $\frac{d\beta}{d\lambda}$. It can be linked to linear dispersion by $dx = f_3 d\beta$ where f_3 is the focal length of the focusing lens. Together with the formula for angular dispersion of a Grism

$$\frac{d\beta}{d\lambda} = \frac{n + dB_1 \sin\frac{\omega}{\lambda^3}}{d\cos\beta} \tag{22}$$

(this formula is taken from [13],the full derivation can be found there as well) the following equation for linear dispersion is found:

$$\frac{d\lambda}{dx} = \frac{d\lambda}{f_3 d\beta} = \frac{1}{f_3} \cdot \frac{d\cos\beta}{n + 2dB_1 \sin\frac{\omega}{\lambda^3}} \tag{23}$$

In the equations above, n is the spectral order, ω is a characteristic of the prism itself, B_1 is one Cauchy's index of refraction coefficient, β is the angle of diffraction, α is the incident angle and d is the grating groove

spacing (so how much space between grooves). However, the width of the exit slit is not known, so the slit width magnification is used to express the width of the exit slit in the width of the entrance slit (for the derivation of this formula see [13]) $w' = w \cdot \frac{cos\alpha}{cos\beta} \cdot \frac{f_3}{f_2}$. Then the equation of the bandpass is found.

$$BP = \frac{w}{f_2} \cdot \frac{d\cos\omega}{n + 2dB_1 \sin\frac{\omega}{\lambda^3}}.$$ (24)

When filling all the values in the figure 2.9 is obtained. It can be seen that the bandpass increases with wavelength. However, it only increases a small amount and at the end of the visible spectrum it is around 0.7nm.
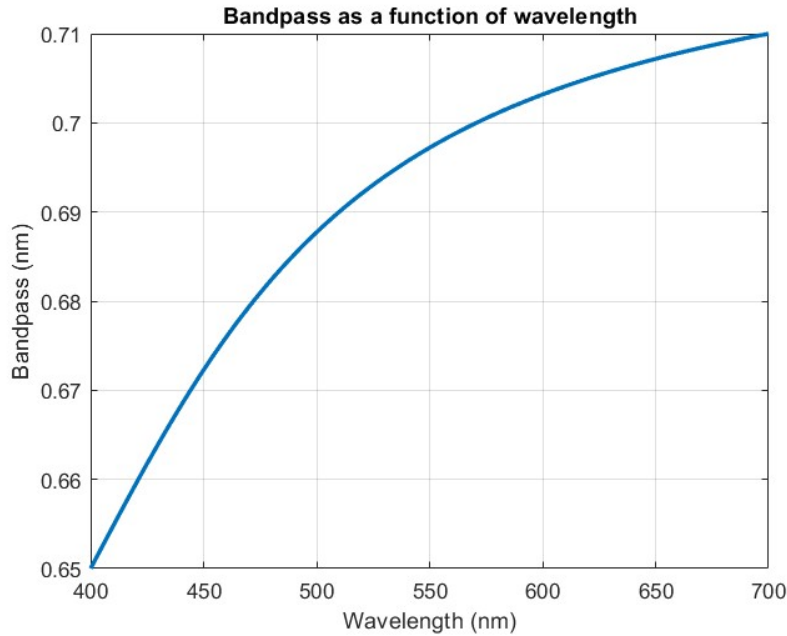
Figure 2.9: Bandpass as a function of wavelength in the visible spectrum.

It is wanted that the BP is as small as possible since then the instrument can distinguish between closely spaced wavelengths and thus its spectral resolution will be higher. However, the theoretically determined value will likely be smaller than the experimentally determined value since there will always be some imperfections in the measuring sequence or equipment. See, figure 2.10 as an example. The intensity on the vertical axis is in arbitrary units. It can be seen that the width at half max (at $I_{max/2}$) is larger for the real instrument than for the ideal instrument, meaning that the bandpass for real instrument is larger than for the ideal instrument as expected.

Taking this into account for MISS 2 and that the bandpass ranges from 0.65nm to 0.71nm in the visible spectrum, it can be said that the real bandpass of miss2 will likely by larger than 1nm.
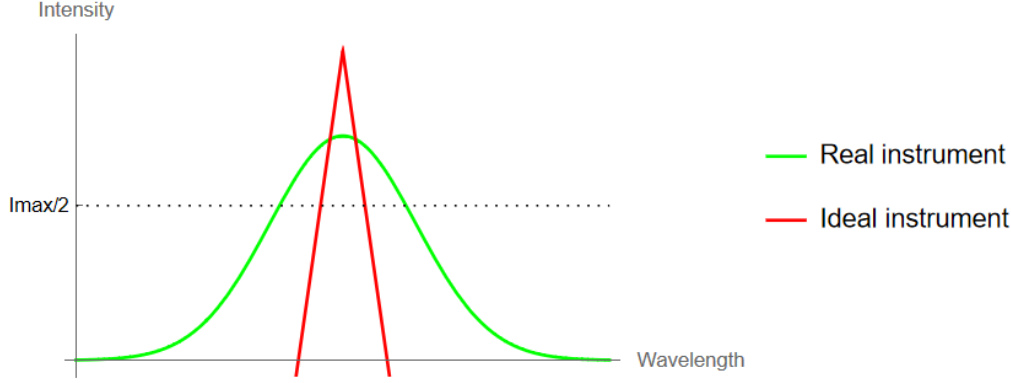
Figure 2.10: Illustration of FWHM, Bandpass, for an ideal instrument (well-alligned) in red and a real instrument in green. The width at half max, $\frac{I_{max}}{2}$ is larger for the real instrument than for the ideal instrument meaning that the spectral resolution for the ideal instrument is better than for the real instrument, as expected. The Intensity is in arbitrary units. Figure based on illustration from [13].

In order to determine the bandpass experimentally, the FWHM is used. Matlab is used to identify the peaks and then determine their widths at half max. The obtained pixel values can then be transformed into wavelengths by the use of equation 2.4.1. Unfortunately, due to lack of time the FWHM is only determined for one calibration spectrogram. This spectrogram was captured when MISS2 was illuminated by a hydrogen alpha lamp with wavelength $\lambda = 656.3$nm. The average of the intensity of the 20 central columns is taken and then the FWHM is determined at 4.9 pixels.

To convert this into wavelengths, the wavelength pixel relation with the calibration coefficients filled in is used. Note: the wavelength is in Ångström here.

$$\lambda(x) = 4088.5 + 2.6739 \cdot (1039 - x) + 1.3462 \cdot 10^{-4} \cdot (1039 - x)^2 \tag{25}$$

First the pixel position, y_c, for wavelength $\lambda_c = 656.3$nm is determined. Then, the pixel positions of each side of the FWHM, $x_1 = x_c - 2.45$ and $x_2 = x_c + 2.45$, are determined. These can then be filled in into equation 2.4.1 and subtracted from each other to find the FWHM $= \lambda(x_2) - \lambda(x_1) = 11.3A = 1.13nm$.

As expected the experimentally determined FWHM is larger than the theoretically determined one. However, it should also be taken into account that for the determination of the experimental FWHM there is only one measurement used and thus it is not extremely reliable. Therefore, if time permits more measurements on FWHM should be done in the future.

2.4.2 Meridian Resolution

The spectrograph captures spectrograms which have on one axis the wavelengths of the visible spectrum and the other axis the whole 180 degree FOV, so from -90 ° to the zenith and back to 90 °. The sensor used, see more in 3.1.7, captures the spectrograms with a resolution of 1391 x 1039 pixels, meaning that 1391 pixels will represent the entire FOV. Therefore, the meridian resolution is $1391/180 = 7.73$ pixels per degree of FOV. However, such precision in meridian direction is not needed since with one pixel per degree FOV the viewed auroras are still good distinguishable. Therefore, one can use binning.

Binning in the context of using a spectrograph, refers to the grouping of adjacent pixels (or spectral channels). So, data of multiple pixels next to each other is combined into one pixel. The main advantage of binning is that this will increase sensitivity. Suppose, one takes four pixels and bins them into one single pixel. This one single pixel will now have the information of the four pixels. So, the light captured for this binned pixel is larger than for a normal pixel. Thus, the sensitivity will go up and that is useful for low light applications like observing aurora. However, the downside of binning is that one loses resolution. But, since the pixels per degree FOV is high using binning could be beneficial using MISS2. For more clarity, figure 2.11 can be viewed. On the left hand-side four pixels with red dots in them representing the light captured. Now, these

pixels are binned into one pixel. As can be seen, the pixel contains now four red dots and thus more light captured in one pixel. Resulting in larger sensitivity and lower resolution.
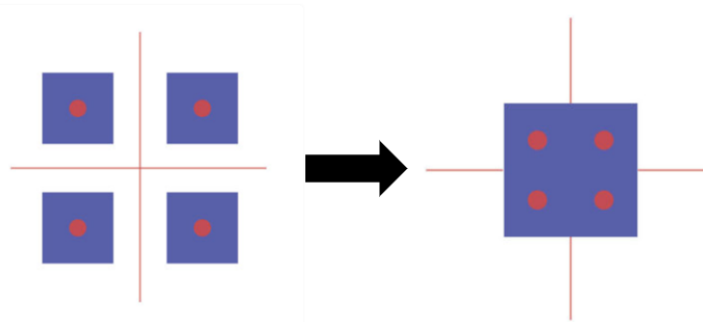
Figure 2.11: Illustration of 2x2 binning, illustration adapted from [21].

2.4.3 Light transmission efficiency

The light captured by MISS 2 is not extremely bright, so the transmission of light inside the spectrograph is of great importance. The spectrograph consists out of multiple components which all have a transmission efficiency below 100 %. In table 2.1 the transmission efficiency of the components used can be seen. Figure 2.12 displays the progressive transmission through the MISS 2. It can be seen that only 20.8 % of the incoming light will reach the sensor. This means that a somewhat long exposure time is needed to make sure enough light will reach the sensor. So, a trade off is needed between the amount of images taken per minute (temporal resolution) and the amount of light reaching the sensor.

Table 2.1: The transmission efficiency off all the separate components. Note: some of the transmission efficiencies are wavelength dependent, in this case 5500 Å has been used. All the data is obtained from the websites of the manufacturers.

Component	Transmission efficiency in %
Peleng all sky lens	70.0
Field lens	91.5
Collimating lens	99.5
Prism	99.0
Grating	55.0
Focusing lens	60.0
Total transmission	20.8
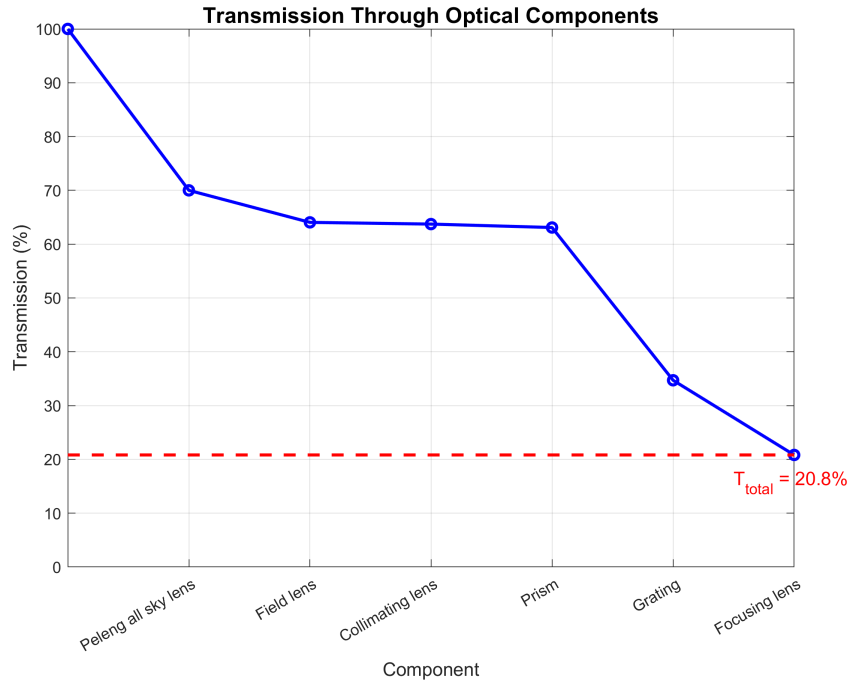
Figure 2.12: Transmission efficiency through all the components of MISS 2.

3 Materials and Methods

In this section all the hardware used in MISS 2 is explained and then the software running on the MISS 2 computer is explained.

3.1 Imaging System

In chapter 2 an example of an optical diagram for a spectrograph was shown, 2.3. The source S is the entire sky and the light will enter the spectrograph by going through an all-sky lens 3.1.1. The all-sky lens will focus the light onto the entrance slit (3.1.2). The light passing the slit will pass a so-called field lens which will minimize losses by ensuring that the light rays leaving the slit will be closer to parallel, so making the light rays less diverging (3.1.3). Now the light rays will be made parallel by the collimating lens (3.1.4) such that they can be properly be dispersed by the dispersive element, a tunable grating in combination with a prism (tGRISM), see section 3.1.5 for more information on the tGRISM. The separated wavelength coming from the tGRISM will be focused by the focusing lens onto the Charge Coupled Device (CCD) sensor.

3.1.1 All-sky lens

An all-sky lens, sometimes called a fisheye lens has a 180 degree field of view (FOV). It is designed to capture an entire hemisphere of the sky in a single image. So, it captures everything from the horizon in all direction to the zenith directly overhead. Thus making it ideal for capturing phenomena spanning large portion of the sky above like aurora, airglow etc. Due to the large FOV there can be distortion occurring near the edges of the horizon but they can be minimized by processing using binning. The all-sky lens used in MISS2 is the Peleng Fisheye made by belOMO, see figure 3.1.

Figure 3.1: The Peleng Fisheye lens made by belOMO. The focal distance is 8 mm and the focusing range is from 0.22 mm to infinity. Photo from Peleng.com

3.1.2 Entrance slit

Behind the Peleng all-sky lens the entrance slit is positioned. This slit ensures that only a specific portion of the light passes through, so only a narrow strip from the entire 180 degree FOV is selected. The width of the entrance slit, w is important since it will influence the spectral resolution and the sensitivity of the whole imaging system. The narrower the slit the less light will enter. This means width of the beam is limited and thus reducing the overlap of adjacent wavelength on the sensor, resulting more distinct spectral lines. However, a narrower slit means the sensitivity will be reduced since less light is entering the. Therefore, one needs to find a balance between spectral resolution and sensitivity.

3.1.3 Field lens

The light which passed through the entrance slit will diverge quite severely. If no field lens would be placed after the entrance slit, the light rays would diverge more causing that not all the light will reach the

collimator resulting in lower efficiency and throughput. But by placing a field lens as close as possible be-
hind the entrance slit the diverging of the lights rays is mitigated and thus improving throughput. The field
lens used in MISS 2 is the Plano-Convex Uncoated by Edmund Optics with an effective focal length of 50mm.

3.1.4 Collimating lens

In order to create parallel rays going to the dispersive element, a collimating lens is placed at it's focal
length after the entrance slit. It is wanted that parallel rays enter the dispersive element since then each
wavelength is diffracted at a consistent angle and thus ensuring that the different wavelengths are separated
evenly. This will produce a clear and well defined spectrum on the sensor. If one doesn't use a collimating
lens the dispersive element would disperse the light in an uncontrolled manner resulting in a blurry/distorted
spectrum. The collimating lens used in MISS2 is AC508-200-A made by Thorlabs with a focal length of 200
mm.

3.1.5 Dispersive Element

As been said in section 2.1.3, a dispersive element will split the incoming light depending on the wavelength.
The dispersive element used in MISS 2 is a Tunable air-spaced Transmission Grating and Prism (tGRISM).
As can be seen in figure 2.5, for the zeroth order all the wavelengths are diffracted to the same spot. But,
the diffraction angle for higher order is wavelength depend. Longer wavelengths such as red have a larger
diffraction angle than colours with smaller wavelength such as blue. For a prism this works the other way
round, colours with longer wavelengths do now have a smaller diffraction angle than colours with smaller
wavelengths. So, if one now uses a grating and a prism together, the light will go more straight through the
design due the opposite working effect of them both.
It is wanted to view the complete visible spectrum (400-700nm) and to achieve this without losing some
wavelengths, it is wanted to have the middle of the spectrum, 550nm, in the middle of the CCD sensor.
Then, all the wavelengths of the visible spectrum are well detectable. One can achieve this by tuning the
grism, so by angular adjustment of the grating (changing the tilt angle) such that the wavelengths are
diffracted at optimal angles allowing the 550nm light to be at the centre of the sensor. See figure 3.2 for how
the light will hit the sensor. The prism used in MISS 2 is a Littrow prism by Altechna and the grating used
is the GT50-06V transmission grating made by Thorlabs.
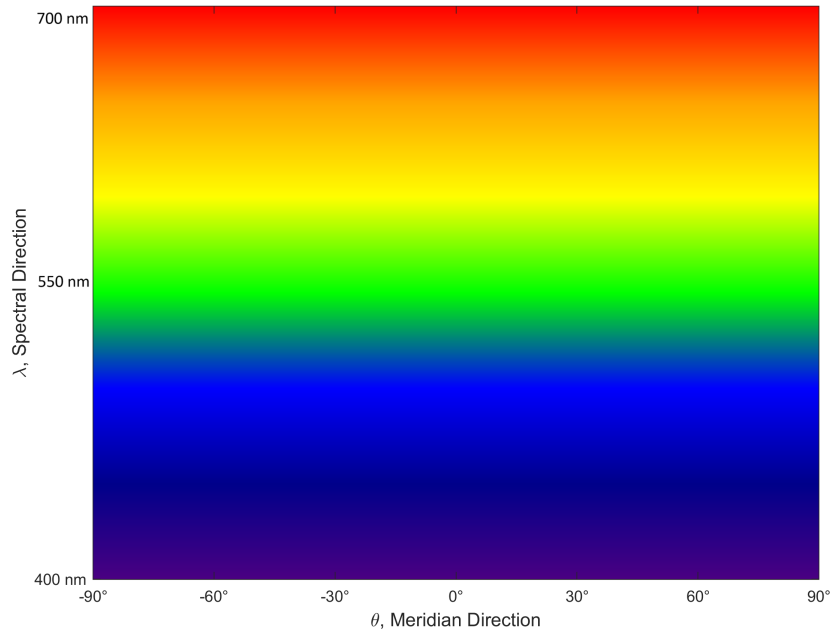
Figure 3.2: The spectrogram with the green colour in the middle of the sensor.

3.1.6 Focusing Lens

The light coming from the grating will be focused on the sensor by a focusing lens. The lens has focal length f_3 such that the projected image uses the surface of the sensor as optimal as possible. The focusing lens used is from Nikon with focal length $f = 35mm$, see figure 3.3.

Figure 3.3: The focusing lens used in MISS2, Nikon Nikkor 35mm, figure from Nikon.

3.1.7 Sensor

The sensor used in MISS 2 is a CCD camera from Atik Cameras, the Atik 414EX with the Sony ICX825 CCD as the sensor, see figure 3.4. A CCD is a sensor which converts light into an electronic signal. It is an ADC (Analog to Digital Converter), so converting an analog signal, in this case the light into a digital signal which can be read out. This sensor has high sensitivity, low noise due to good cooling capabilities and thus making it suitable to capture low light phenomena such aurora. The sensor will capture spectrograms looking like figure 3.2. The resolution of is 1391 x 1039 pixels, so when a spectrogram is captured the image is converted into a grid of 1391 x 1039 pixels. As shown in figure 3.2 , the wavelengths in the visible spectrum

are represented on the vertical axis. Thus, 1039 pixels represent a 300nm range of wavelengths resulting in that wavelengths closer than 300nm/1039= 0.289nm to each other can not be resolved by the sensor. For the horizontal axis there are 1391 pixels representing a 180 degree FOV, resulting in 1391/180=7.73 pixels per degree. But, there is no need for finer resolution than one degree for MISS2. This means one could use binning in order to increase the sensitivity without losing the meridian information, see section 2.4.2 for more information on binning.

Figure 3.4: The Atik 414EX camera, figure from Atik cameras.

3.1.8   MISS2 assembled

In the figure 3.5 MISS2 can be seen installed at KHO in one of the domes. MISS2 is placed on a solid aluminium optical breadboard and then screwed onto a special made wooden structure (handmade by professor Sigernes and the author).

Figure 3.5: MISS 2 installed at KHO in the down, to the left of MISS2 there is a normal photocamera.

3.2 Software

The software running on the MISS 2 is based on the software running on MISS 1. The software principles of MISS 2 were developed by Nicolas Martinez from Luleå Tekniska Universitet and extended such that MISS 2 can run continuously without human interference by the author. The software is designed such that aurora can be tracked. The software is split up in two parts, capturing data and processing data. The processing is done continuously, so every five minutes the programs are ran from start and thus processing data continuously. From all the programs used for real time processing there are also programs made which asks a date as input from the user and the program will then process all the data found for that specific date. For the exact programs visit: https://github.com/JesseTUe/KHO-MISS .

3.2.1 Capturing data

The main program which controls the camera is called: CaptureAtik.py, see figure 3.6 for a flow diagram of the program. First, the program retrieves the relevant data from the parameters file (this file contains relevant directories, camera settings, calibration coefficients etc.) after which it checks if the sun is lower than 10 degrees under the horizon, if not it will check again after 30 seconds and if yes then it proceeds. Then it tries to connect to the Atik camera (the sensor), if the connection is successful it prints the device name and returns the camera object. If the connection fails, the program will retry after 30 seconds. After connecting the program sets the relevant parameters: exposure duration, binning factors and cooling temperature of the CCD. If wanted by the user the images are rescaled according to a certain threshold inputted by the user. This can be handy if the intensities are really low and badly visible. Lastly, the captured image is saved with the relevant metadata i.e. Exposure duration, binning, temperature, date and time. The number of spectrograms captured per minute depends on the imaging cadence parameter, given as input by the user in the parameters file. Currently, this is set to 15 seconds meaning that four images per minute are captured.
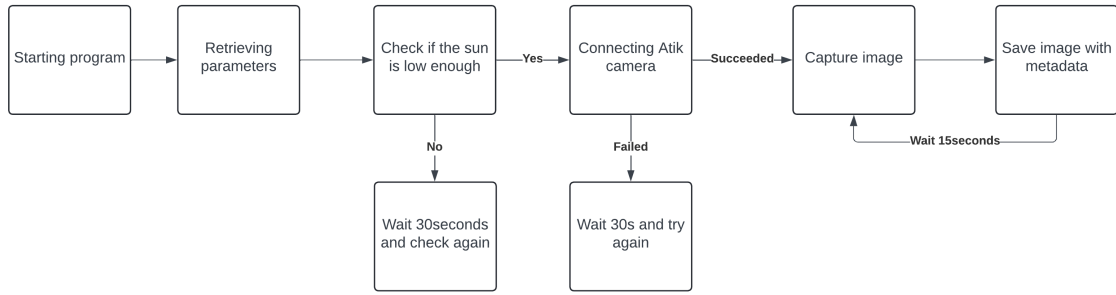
Figure 3.6: Workflow of the capturing images program.

3.2.2 Data processing

The captured images (spectrograms) by the CaptureAtik program explained above are first averaged minute wise since this saves processing power. From these averaged spectrograms, processed spectrograms and RGB columns will be made. Out of these RGB columns a keogram is made and together with the processed spectrograms published on the KHO website. This sequence is performed every five minutes, so every five minutes the data on the KHO website is updated if MISS 2 is active, see 3.7 for the workflow of the data processing. These separated programs will be discussed below.
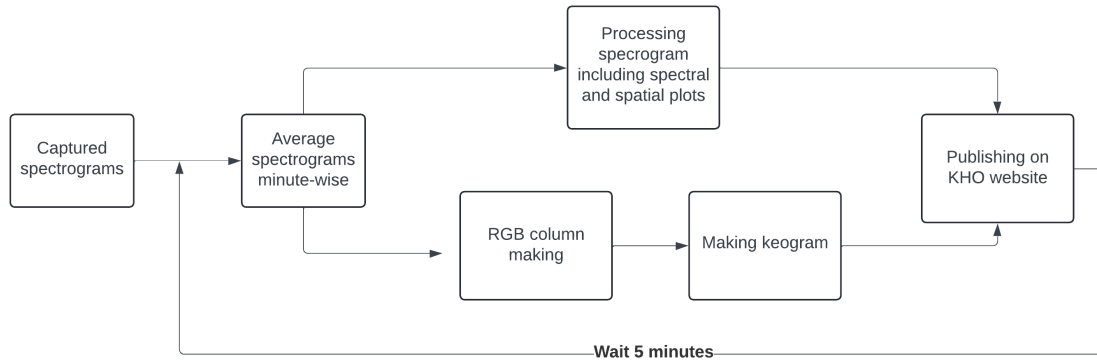
Figure 3.7: Workflow of the processing of the captured spectrograms.

Minute-wise averaged spectrogram maker

This program will first check if there are any spectrograms captured for the last five minutes. Then it will group them by the minute and for each minute group it will average the pixel intensities across the spectrogram. Also, metadata is added after which it is saved. In order to avoid duplicate processing a record is maintained of the processed minute groups.
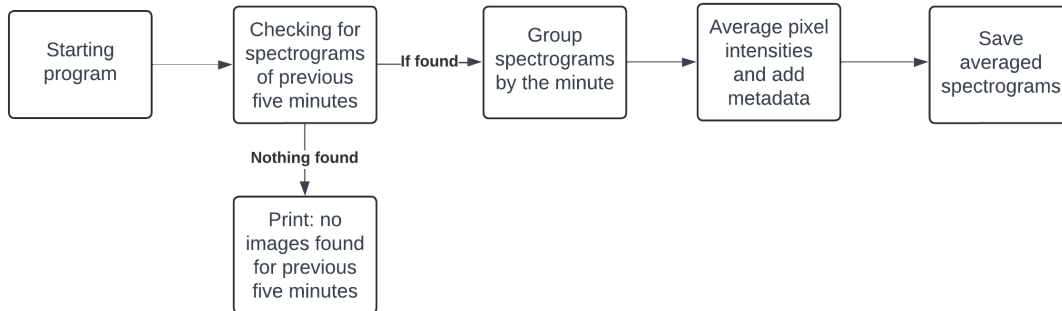
Figure 3.8: Workflow of the minute-wise average spectrogram program.

Spectrogram Processing

This program processes minute averaged spectrograms by applying transformations and calibrations. Out of the averaged spectrograms spectral and spatial data is extracted, plotted and published.
First, the minute averaged spectrograms from the last five minutes are extracted from the indicated directory. Then, the spectrogram is flipped and rotated by 90 degrees to correct for orientation and align with the wavelength axis. Subsequently, the median intensity is obtained by taking the median of each column and subtracting this background from the image to minimize noise. Now, the wavelength calibration is performed to determine the wavelength for each pixel column in the averaged spectrogram, using the calibration coefficient obtained by performing calibration measurements in the lab (these calibration are done by Nicolas Martinez). Afterwards, radiometric calibration is done to obtain the actual radiance from the pixel intensity. Then, the spectrogram is plotted with two subplots, a spectral analysis plot displaying the spectral radiance in kR/Å across the wavelengths and a spatial analysis plot showing the radiance in kR/θ across the elevation angles.
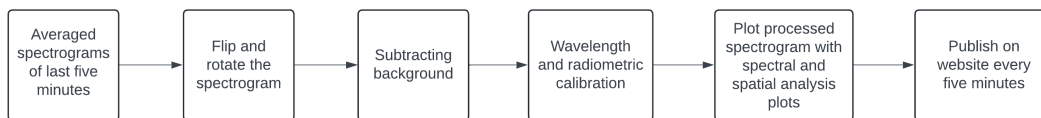
Figure 3.9: Workflow of the spectrogram processing.

RGB column making

This program processes the minuted averaged spectrograms in order to generate Red Green Blue (RGB) columns which represent the specific auroral emission lines. The RGB columns are created by extracting data for the three auroral emission wavelengths, 6300Å, 5577Å and 4278Å corresponding to red, green and blue respectively. 6300Å represents the oxygen emission line and occurs when oxygen transitions from an excited state to a lower energy state. It occurs at an altitude of around 200-300km above the earth. 5577Å also represents an oxygen emission line but at lower altitudes, around 100-150km above the earth. Lastly, 4278Å represents the nitrogen ion (N_2^+) emission line and can be seen around 120km above the earth.

First, the program checks for averaged spectrograms in the last five minute and retrieves the necessary metadata and coefficients. Then the specific pixel rows where auroral emission appears are determined by using the wavelength pixel relation, so the wavelengths of the auroral emission are linked to pixel positions. If these emission line positions are then successfully determined, each emission line is normalized and reshaped to create a column with the following shape, (300, 1, 3). So, 300 pixels vertical, one horizontal and three columns stacked. The RGB columns are then saved with the correct UTC (=Coordinated Universal Time).

```
┌──────────────┐   ┌──────────────┐   ┌──────────────┐   ┌──────────────┐   ┌──────────────┐
│  Averaged    │   │   Using      │   │Pixel rows    │   │Normalization │   │RGB column    │
│ spectrograms │──▶│ wavelength   │──▶│linked to     │──▶│and           │──▶│with          │
│ of last five │   │pixel relation│   │RGB emission  │   │reshaping     │   │shape(300,1,3)│
│   minutes    │   │              │   │lines         │   │              │   │              │
└──────────────┘   └──────────────┘   └──────────────┘   └──────────────┘   └──────────────┘
```
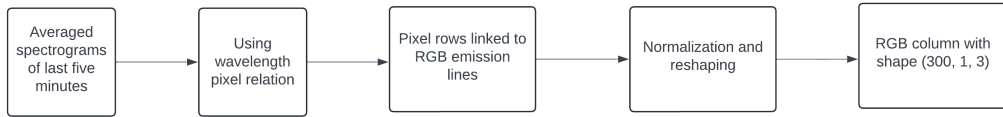
Figure 3.10: Workflow of the RGB column making process.

Keogram making

A keogram is a way to visualize spatial and temporal variations in atmospheric phenomena. So, by making RGB columns per minute and putting them behind each other a keogram is made.
The program initializes an keogram filled with white pixels. Then, all the RGB images from midnight until current UTC are gathered and put in the keogram. Then, the keogram is published on the KHO website.

```
┌──────────────┐   ┌──────────────┐   ┌──────────────┐   ┌──────────────┐
│ Initialize a │   │Gather all the│   │ Filling the  │   │  Publish     │
│   keogram    │   │    RGB       │   │keogram with  │   │ keogram on   │
│  filled with │──▶│  columns of  │──▶│  the RGB     │──▶│website every │
│ white pixels │   │   the day    │   │  columns     │   │five minutes  │
└──────────────┘   └──────────────┘   └──────────────┘   └──────────────┘
```
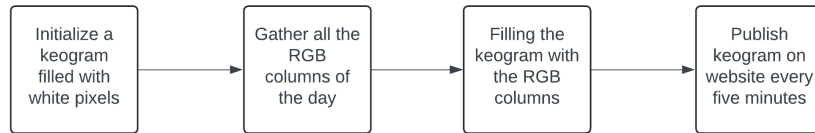
Figure 3.11: Workflow of making a keogram.

4 Results

In this section the obtained spectrogram and keograms will be shown and compared to other instruments present at the KHO.

4.1 Processed Spectrogram

In figure 4.1 in the middle a processed spectrogram can be seen of the evening of 30 October 2024. At the top there is graph which shows the radiance per wavelength (spectral analysis) and to the side there is graph which shows the radiance per degree of elevation (spatial analysis). In the spectrogram there is one line clearly visible and one line reasonable visible across the whole elevation. The brighter a part of the line gets in the spectrogram, the higher the radiance is at this location. This bright line represents the green aurora, as can be seen from the spectral analysis plot. The reasonable visible line represents the red aurora. According to the spatial analysis the aurora occured across the whole meridian but was a bit brighter at some parts than the other parts.
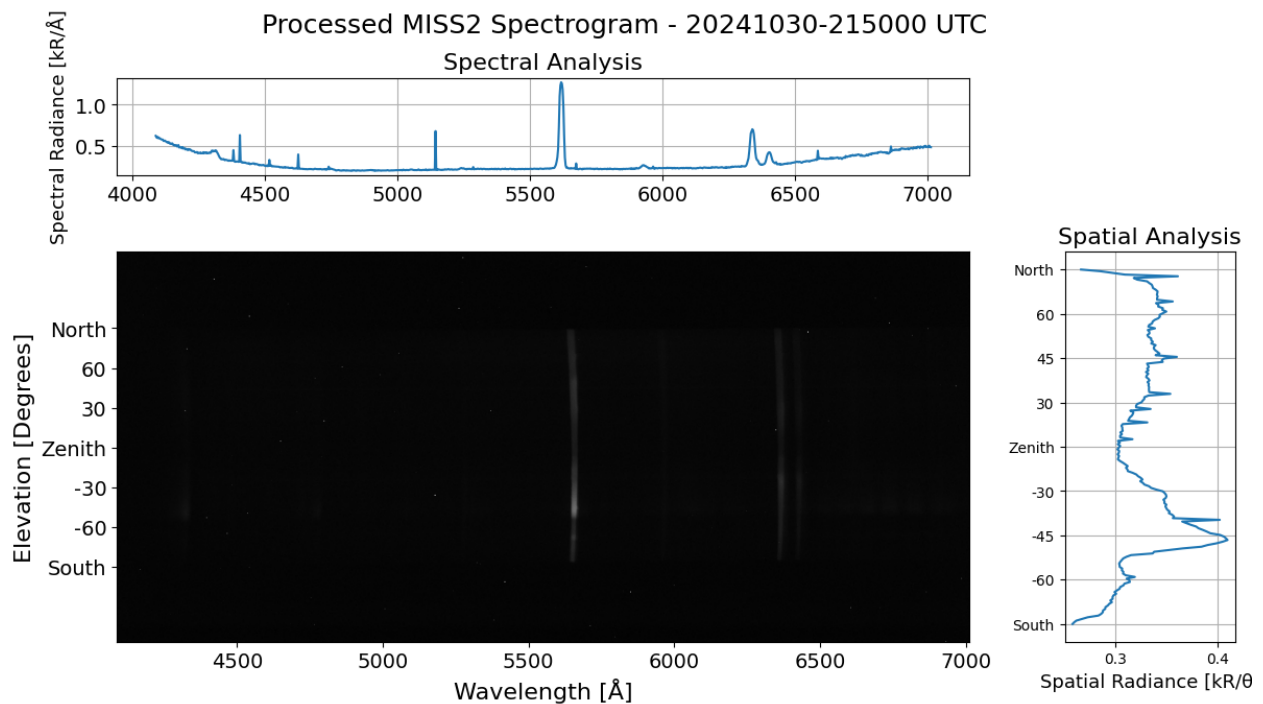
Figure 4.1: A processed spectrogram with a spectral analysis plot and a spatial analysis plot.

In order to check if there was actually aurora at this time and thus if MISS2 is working as it supposed to, we take a look at the captured keogram by the Sony A7 all-sky camera installed at the KHO, see figure 4.2. As can be seen, around 21:00UTC to 22:30UTC there has been some nicely visible aurora.
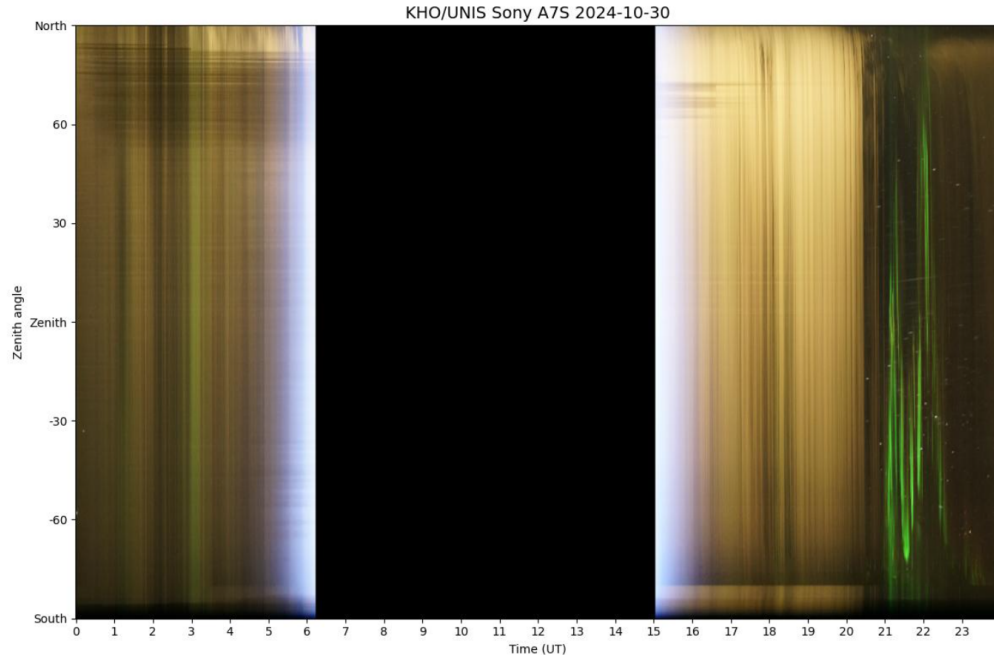
Figure 4.2: Keogram of 30 October 2024 made by the Sony A7 all-sky camera at KHO. Figure from kho.unis.no.

4.2   Keogram

In order to give a quick summary of the auroral activity of a day, a keogram can be viewed. As explained in section 3.2.2, the keograms are made out of RGB columns made by using the auroral emission lines. In figure 4.3 the keogram of 30 October 2024 made by MISS2 can be seen.

The colours in the keogram are not correct yet and this is work in progress (the author tried his best to finetune the colours but wasn't able to make it better). But, the promising thing is that if one looks closely to the timeframe where aurora is visible (around 21:00 - 22:00 UTC) the aurora is visible but in the wrong colours.
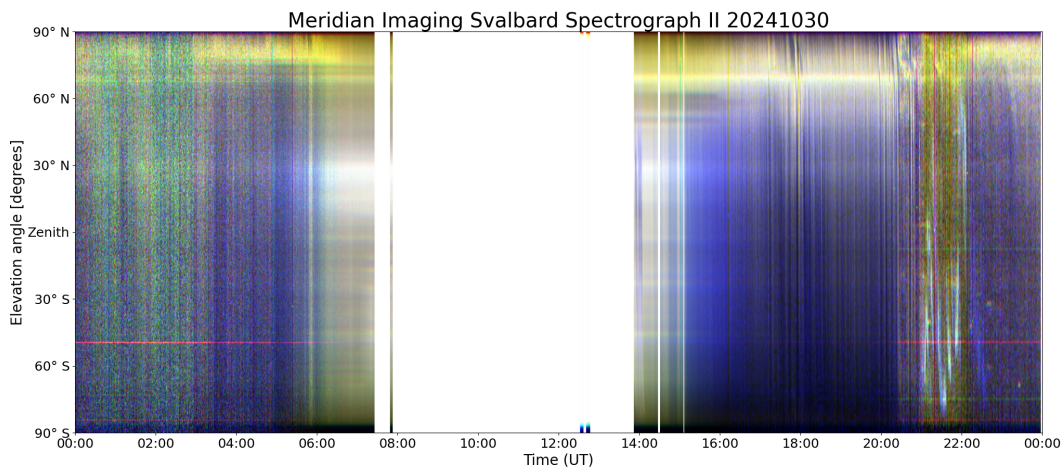
Figure 4.3: Keogram of 30th October 2024 made by the MISS2. Colours are not correct yet.

25

5 Conclusion

The aim of this project was to install and operationalize the Meridian Imaging Svalbard Spectrograph 2 at the Kjell Henriksen Observatory such that it could be used to track aurora in the upcoming dark season. This is done by adjusting/improving the software used for calibration. MISS 2 is placed at the KHO due to its great location close to the magnetic north pole. The Field Of View of the spectrograph is 180 degrees so making it perfect for observing aurora along the geomagnetic meridian plane from North to South.

MISS 2 is capturing four raw spectrograms per minute when the sun is 10 degrees below the horizon. These spectrograms are then processed and plotted together with a spectral and spatial analysis. The green aurora has correctly been observed. Out of these raw spectrograms RGB columns are made based on the auroral emission lines (Red 630 nm, Green 557.8 nm and Blue 427.7 nm) which are plotted behind each other to make a keogram. The keograms made by MISS 2 show that there has been aurora but do not show the right colours unfortunately. It was tried to solve this problem but due to lack of time the cause of the problem was not found yet.

Overall, the project outcome was a success since the goal of operationalizing MISS 2 is achieved and the data is published on the website of the observatory (https://kho.unis.no/data/MISS2.html), but the were also things which could have been done better. As mentioned, the colouring of the RGB columns was not as it should be. The most obvious cause is that there is an error made by the author in the software, i.e. incorrect use of the wavelength pixel relation, incorrect use of background subtraction, scaling of the of the columns into the correct form (300, 1, 3), wavelength or sensitivity coefficients are a bit off etc. However, most of the aforementioned causes are checked by the author and nothing seemed odd. Another plausible cause is that the colours are not correctly fine-tuned, so the RGB values are not well balanced. As can be seen in the keogram presented, large parts look blue. It has been briefly tried to solve this issue but with little to no success. The research group of professor Sigerness will continue with the investigation of the problem and hopefully find a solution for the weird colouring.

Also, there could have also be done more characterization to get a better idea of the bandpass when viewing aurora since now only the bandpass is determined experimentally for one measurement which was taken during calibration.

Now that MISS 2 is operational, the software developed will also be put on MISS 1. This will create the opportunity to do comparisons and providing more extensive insights into aurora and especially when MISS 1 will be installed at Ny-Ålesund.

References

[1] C.T. Russell, J.G. Luhmann, and R.J. Strangeway. *Space Physic, An Introduction*. Cambridge University Press, 2016.

[2] Robert Marc Friedman. Making sense of the aurora: A research project. *Nordlit*, (no. 29):59–68, 2012.

[3] T. A. Potemra. Observation of birkeland currents with the triad satellite. *Astrophysics and Space Science*, sep 1978.

[4] Thomas A. Potemra. Field-aligned (birkeland) currents. *Space Science Reviews*, dec 1985.

[5] C. R. Clauer and A. J. Ridley. Ionospheric observations of magnetospheric low-latitude boundary layer waves on august 4, 1991. *Geophys. Res.*, 1995.

[6] R. G. ROBLE and E. C. RIDLEY. An auroral model for the ncar thermospheric general circulation model (tgcm). *Annales Geophysicae, Series A - Upper Atmosphere and Space Sciences*, dec 1987.

[7] Stephen B. Mende. Observing the magnetosphere through global auroral imaging: 2. observing techniques. *JGR Space Physics*, sep 2016.

[8] Gladimir V. G. Baranoski, Jon G. Rokne, Peter Shirley, Trond S. Trondsen, and Rui Bastos. Simulating the aurora. *The Journal of Visualization and Computer Animation*, feb 2003.

[9] José Manuel Amigo. Chapter 1.1 - hyperspectral and multispectral imaging: setting the scene. *Data Handling in Science and Technology*, sep 2019.

[10] Andrew Bodkin, A. Sheinis, A. Norton, J. Daly, S. Beaven, and J. Weinheimer. Snapshot hyperspectral imaging – the hyperpixel array™ camera. *SPIE*, apr 2009.

[11] Alexander F.H. Goetz. Three decades of hyperspectral remote sensing of the earth: A personal view. *Remote Sensing of Environment*, dec 2007.

[12] Charles A. Bennet. *Principles of Physical Optics*. Wiley, first edition, sep 2008.

[13] Fred Sigernes. Hyper spectral imaging, 2018.

[14] Marie Bøe Henriksen. Hyperspectral imager calibration and image correction. Master's thesis, Norwegian University of Science and Technology, jun 2019.

[15] Paul Quincey. Solid angles in perspective. *Physics Education*, 2020.

[16] Christopher Palmer. *Diffraction Grating Handbook*. MKS Newport, eighth edition, 2020.

[17] Edmund Optics. All about diffraction gratings, 2024.

[18] Long Que, Chester G. Wilson, and Yogesh B. Gianchandani. Microfluidic electrodischarge devices with integrated dispersion optics for spectral analysis of water impurities. *Journal Of Microelectromechanical Systems*, apr 2005.

[19] The European Space Agency. Hyperspectral image cube showing mount vesuvius, italy, 2021.

[20] Japan Association of Remote Sensing. Remote sensing notes, 1999.

[21] Jacob from Atik Cameras. Binnning: The differences between cmos and ccd, dec 2017.

Appendix (A)